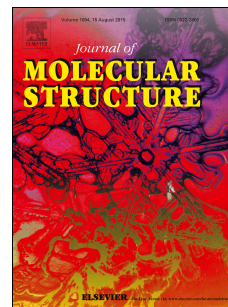


Accepted Manuscript

Syntheses, structural characterization, luminescence and optical studies of Ni(II) and Zn(II) complexes containing salophen ligand

M.S. More, S.B. Pawal, S.R. Lolage, S.S. Chavan



PII: S0022-2860(16)30913-9

DOI: [10.1016/j.molstruc.2016.08.083](https://doi.org/10.1016/j.molstruc.2016.08.083)

Reference: MOLSTR 22909

To appear in: *Journal of Molecular Structure*

Received Date: 13 May 2016

Revised Date: 31 August 2016

Accepted Date: 31 August 2016

Please cite this article as: M.S. More, S.B. Pawal, S.R. Lolage, S.S. Chavan, Syntheses, structural characterization, luminescence and optical studies of Ni(II) and Zn(II) complexes containing salophen ligand, *Journal of Molecular Structure* (2016), doi: 10.1016/j.molstruc.2016.08.083.

This is a PDF file of an unedited manuscript that has been accepted for publication. As a service to our customers we are providing this early version of the manuscript. The manuscript will undergo copyediting, typesetting, and review of the resulting proof before it is published in its final form. Please note that during the production process errors may be discovered which could affect the content, and all legal disclaimers that apply to the journal pertain.

Graphical Abstract:**Syntheses, structural characterization, luminescence and optical studies of Ni(II) and Zn(II) complexes containing salophen ligand**

M. S. More, S. B. Pawal, S. R. Lolage, S. S. Chavan*

Department of Chemistry, Shivaji University, Kolhapur (MS), India-416 004

Abstract

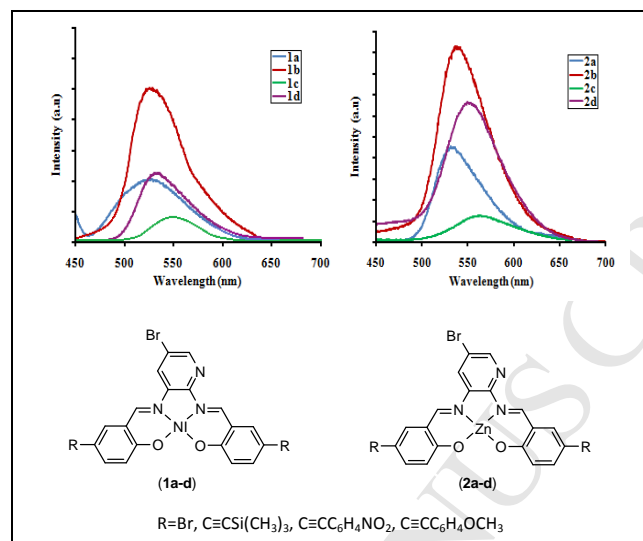
Some Ni(II) (**1a-d**) and Zn(II) (**2a-d**) salophen complexes have been prepared and characterized. X-ray diffraction of **1c** and **2b** and SEM studies of **1b** and **2d** are used to elucidate the crystal structure and morphology of the complexes. All complexes exhibit a distinct MLCT absorption band and shifted to longer wavelength by increasing π -conjugation in the complexes. Room temperature luminescence is observed for all complexes in DMF which is finely tuned by the degree of extended π -conjugation and variation of the substituent group with different electronic effects in the complexes. The second harmonic generation (SHG) efficiency of the complexes was screened by Kurtz-powder technique indicating that all complexes possess promising potential application as a useful NLO material.

Keywords: Ni(II)/Zn(II)-salophen complexes, photoluminescence, optical properties

Corresponding author: Tel.: +91 231 2609381; fax: +91 231 2691533.

E-mail: sanjaycha2@rediffmail.com

Graphical Abstract: Pictogram



Syntheses, structural characterization, luminescence and optical studies of Ni(II) and Zn(II) complexes containing salophen ligand

M. S. More, S. B. Pawal, S. R. Lolage, S. S. Chavan*

Department of Chemistry, Shivaji University, Kolhapur (MS), India-416 004

Abstract

Some Ni(II) (**1a-d**) and Zn(II) (**2a-d**) salophen complexes were prepared by the treatment of 5-bromo salicylaldehyde, 5-(trimethylsilylethynyl)salicylaldehyde, 5-(4-nitrophenyl)ethynylsalicylaldehyde or 5-(4-methoxyphenyl)ethynylsalicylaldehyde with nickel acetate or zinc acetate followed by addition of 2,3-diamino-5-bromopyridine. All complexes were characterized by elemental analyses, IR, ¹H NMR and mass spectral studies. X-ray powder diffraction of representative complexes **1c** and **2b** and SEM studies of **1b** and **2d** are used to elucidate the crystal structure and morphology of the complexes. The electrochemical behavior reveals that the redox responses of Ni(II) complexes shifted to more negative potential in order to increase the π -conjugation in the complexes. Room temperature luminescence is observed for all complexes corresponding to $\pi \rightarrow \pi^*$ ILCT transition with some MLCT character in DMF and is finely tuned by the degree of extended π -conjugation and variation of the substituent group with different electronic effects in the complexes. The second harmonic generation (SHG) efficiency of the complexes was screened by Kurtz-powder technique indicating that all complexes possesses promising potential for the application as a useful nonlinear optical material.

Keywords: Ni(II)/Zn(II)-salophen complexes, photoluminescence, optical properties

Corresponding author: Tel.: +91 231 2609381; fax: +91 231 2691533.

E-mail: sanjaycha2@rediffmail.com

1. Introduction

Transition metal complexes with salophen type ligand have attracted enormous attention in coordination chemistry due to their structural liability, unusual configuration and sensitivity towards environment as a functional material [1-3]. The important feature of these system is that salophen ligand offering a tetradentate chelating system to form a stable complexes and thus they have strong $\pi \rightarrow \pi^*$ intermolecular interactions. They are known to act as an efficient catalyst both in homogeneous and heterogeneous reactions for asymmetric ring-opening of epoxides, aziridination, cyclopropanation, oxidation, reduction reaction of ketones, epoxidation of olefins, formation of cyclic and linear polycarbonates, catalytic enantioselective and diastereoselective redox reactions and Diels-Alder reactions [4-7]. They become an efficient entities to study the interactions with DNA, leading to the development of sensitive chemical probes for DNA [8]. Applications of transition metal-salophen complexes also have been explored in material sciences such as nonlinear optical (NLO) properties due to their potential applications in optoelectronic devices of information storage, telecommunications, signal processing etc. [9-11]. Moreover, they are known to act as an excellent candidate as a luminescent material with possible utilization in solar energy conversion, luminescent sensors, electroluminescent sensors and probes for biological systems [12-14]. The source of their luminescence is due to the metal to ligand charge transfer (MLCT) excited state, which is usually sensitive to molecular configuration and peripheral ligand. Owing to their wide utility in various fields and its ability to act as polyfunctional ligand many studies on coordination behavior of salophen ligand with transition metal ions have been carried out [15-17]. In recent years considerable research efforts have been focused on incorporation of additional functionalities into coordinating ligand which are reported to exhibit very interesting luminescent and optical properties [18, 19]. The incorporation of additional functionality into coordinating ligand and

their metal complexes was found to destabilize non-radiative d-d transitions to maintain the structural integrity and thus displaying reasonable luminescence properties. Addition of alkynyl functionality particularly, with a π -conjugation constitutes an important class of compounds as a luminescent material due to their advanced electronic and structural properties [20]. An important feature of these system is the structural modification which causes a larger π -delocalization over the salophen ligand than that of the regular complexes. Moreover, rigidity of the structure and the dipole moment of the complexes may thus increase.

Influenced by these facts and to study the effect of a π -conjugation and donor-acceptor substituent's of salophen ligand, it was considered worthwhile to undertake synthesis of some Ni(II) (**1a-d**) and Zn(II) (**2a-d**) salophen complexes by treatment of 5-bromosalicylaldehyde, 5-(trimethylsilylethynyl)salicylaldehyde, 5-(4-nitrophenyl)ethynylsalicylaldehyde or 5-(4-methoxyphenyl)ethynylsalicylaldehyde with nickel acetate or zinc acetate followed by addition of 2,3-diamino-5-bromopyridine. All the complexes have been characterized by elemental analysis and several spectroscopic techniques. The photoluminescence, redox behavior and SHG efficiency of the complexes have been reported.

2. Experimental

2.1. Materials and measurements

All chemicals used were of AR grade. Solvents used for synthesis were distilled over appropriate drying reagents. 5-(trimethylsilylethynyl)salicylaldehyde, 5-(4-nitrophenylethynyl)salicylaldehyde and 5-(4-methoxyphenyl)ethynylsalicylaldehyde were prepared by following the procedure reported in the literature [21]. ^1H NMR spectra were recorded on Bruker 300 MHz instrument using TMS [$(\text{CH}_3)_4\text{Si}$] as an internal standard and were reported with residual protons in the solvent as standard (d_6 -methylsulfoxide, δ 2.50). ESI mass spectra were recorded on JEOL SX-102A spectrometer. Elemental

analyses (C, H and N) were performed on a Thermo Finnigan FLASH EA-112 CHNS analyzer. Absorption spectra were recorded on a Shimadzu UV-Vis-NIR-100 spectrophotometer. Infrared spectra were performed on a Perkin-Elmer FT-IR spectrometer using KBr pellets in the 4000-450 cm^{-1} spectral range. Thermal analysis of the complexes was carried out on a Perkin Elmer thermal analyzer in nitrogen atmosphere at a heating rate of 10 $^{\circ}\text{C}/\text{min}$. Luminescence properties were measured using a Perkin Elmer fluorescence spectrometer LS-55. Luminescence lifetime measurements were carried out by using time-correlated single photon counting from HORIBA Jobin Yvon. X-ray powder diffraction was carried out by using D2 PHASER-X-ray powder diffractometer operated by using $\text{CuK}\alpha$ line at 1.54056 \AA as the radiation source. The surface morphology of prepared complexes were analyzed using scanning electron microscope (SEM) in which the images were acquired by using the JEOL JSM-6360. Cyclic voltammetry measurements were performed with a CH-400A electrochemical analyzer. A standard three electrode system, consisting of Pt disk working electrode, Pt wire counter electrode and Ag/AgCl reference electrode were used. All potentials were converted to SCE scale. Tetrabutyl ammonium perchlorate (TBAP) was used as a supporting electrolyte and all measurements were carried out in DMF solution at room temperature with scan rate 100 mVs^{-1} .

2.2. Synthesis of Ni(II)-salophen complexes (**1a-d**)

5-bromosalicylaldehyde (0.342 mmol, 0.0688 g), 5-(trimethylsilylethynyl)salicylaldehyde (0.342 mmol, 0.0747 g), 5-(4-nitrophenyl)ethynylsalicylaldehyde (0.342 mmol, 0.0915 g) or 5-(4-methoxyphenyl)ethynylsalicylaldehyde (0.342 mmol, 0.0863 g) was first treated with $\text{Ni}(\text{OAc})_2 \cdot 4\text{H}_2\text{O}$ (0.171 mmol, 0.0426 g) and the mixture was stirred in CH_2Cl_2 :THF (20 ml:10 ml) for 30 min. at room temperature. 2,3-diamino-5-bromopyridine (0.171 mmol, 0.0322 g) in THF (10 ml) was added to the resulting solution and the mixture was stirred overnight. The solvent was then removed by *vacuum* and the solid complex precipitated was collected by filtration, washed with 1:1 ethanol:water mixture and dried under *vacuum* at room temperature.

1a: Yield: 78 %; elemental analyses (C, H and N, wt %) Anal. Calc. for $C_{19}H_{10}N_3O_2Br_3Ni$: C, 37.37; H, 1.65; N, 6.88 found: C, 37.18; H, 1.47; N, 6.93; IR (KBr, cm^{-1}): 1608, $\nu(HC=N)$; 1293, $\nu(C-O)$; 1H NMR (d_6 -DMSO, 300 MHz): δ 9.37 (s, 1H, HC=N), δ 9.16 (s, 1H, HC=N), δ 6.65-8.67 (m, 8H, Ar-H); MS (ESI): m/z 633 (M+Na) $^+$. **1b:** Yield: 82%; elemental analyses (C, H and N, wt %) Anal. Calc. for $C_{29}H_{28}N_3O_2BrSi_2Ni$: C, 53.97; H, 4.37; N, 6.51; found: C, 53.79; H, 4.26; N, 6.58; IR (KBr, cm^{-1}): 2140, $\nu(C\equiv C)$; 1609, $\nu(HC=N)$; 1296, $\nu(C-O)$; 1H NMR (d_6 -DMSO, 300 MHz): δ 9.35 (s, 1H, HC=N), δ 9.19 (s, 1H, HC=N), δ 6.67-8.29 (m, 8H, Ar-H), δ 0.26 (s, 18H, $(CH_3)_3Si$); MS (ESI): m/z 668 (M+Na) $^+$. **1c:** Yield: 79%; elemental analyses (C, H and N, wt %) Anal. Calc. for $C_{35}H_{18}N_5O_6BrNi$: C, 56.57; H, 2.44; N, 9.42; found: C, 56.49; H, 2.37; N, 9.51; IR (KBr, cm^{-1}): 2201, $\nu(C\equiv C)$; 1615, $\nu(HC=N)$; 1334, $\nu(C-O)$; 1H NMR (d_6 -DMSO, 300 MHz): δ 9.39 (s, 1H, HC=N), δ 9.14 (s, 1H, HC=N), δ 6.75-8.69 (m, 16H, Ar-H); MS (ESI): m/z 766 (M+Na) $^+$. **1d:** Yield: 77 %; elemental analyses (C, H and N, wt %) Anal. Calc. for $C_{37}H_{24}N_3O_4BrNi$: C, 62.31; H, 3.39; N, 5.89; found: C, 62.22; H, 3.27; N, 5.96; IR (KBr, cm^{-1}): 2197, $\nu(C\equiv C)$; 1613, $\nu(HC=N)$; 1282, $\nu(C-O)$; 1H NMR (d_6 -DMSO, 300 MHz): δ 9.38 (s, 1H, HC=N), δ 9.13 (s, 1H, HC=N), δ 6.73-8.61 (m, 16H, Ar-H), δ 3.74 (s, 6H, OCH_3); MS (ESI): m/z 736 (M+Na) $^+$.

2.3. Synthesis of Zn(II)-salophen complexes (**2a-d**)

5-bromosalicylaldehyde (0.392 mmol, 0.0789 g), 5-(trimethylsilylethynyl)salicylaldehyde (0.392 mmol, 0.0856 g), 5-(4-nitrophenyl)ethynylsalicylaldehyde (0.392 mmol, 0.1049 g) or 5-(4-methoxyphenyl)ethynylsalicylaldehyde (0.392 mmol, 0.0991 g) was first treated with $Zn(OAc)_2 \cdot 2H_2O$ (0.196 mmol, 0.0431 g) and the mixture was stirred in CH_2Cl_2 :THF (20 ml : 10 ml) for 30 min. at room temperature. 2,3-diamino-5-bromopyridine (0.196 mmol, 0.0369 g) in THF (10 ml) was added to the resulting solution and the mixture was stirred overnight. Then the solvent was removed by *vacuum* and the solid complex precipitated was collected by filtration, washed with 1:1 ethanol:water mixture and dried under *vacuum* at room temperature.

2a: Yield: 75 %; elemental analyses (C, H and N, wt %) Anal. Calc. for $C_{19}H_{10}N_3O_2Br_3Zn$: C, 36.96; H, 1.63; N, 6.81; found: C, 36.78; H, 1.57; N, 6.89; IR (KBr, cm^{-1}): 1608, $\nu(HC=N)$; 1279, $\nu(C-O)$; 1H NMR (d_6 -DMSO, 300 MHz): δ 9.36 (s, 1H, HC=N), δ 9.21 (s, 1H, HC=N), δ 6.67-8.21 (m, 8H, Ar-H); MS (ESI): m/z 635 ($M+Na$)⁺. **2b:** Yield: 69 %; elemental analyses (C, H and N, wt %) Anal. Calc. for $C_{29}H_{28}N_3O_2BrSi_2Zn$: C, 53.42; H, 4.33; N, 6.44; found: C, 53.26; H, 4.24; N, 6.62; IR (KBr, cm^{-1}): 2149, $\nu(C\equiv C)$; 1606, $\nu(HC=N)$; 1278, $\nu(C-O)$; 1H NMR (d_6 -DMSO, 300 MHz): δ 9.34 (s, 1H, HC=N), δ 9.29 (s, 1H, HC=N), δ 6.69-8.26 (m, 8H, Ar-H), δ 0.26 (s, 18H, $(CH_3)_3Si$); MS (ESI): m/z 675 ($M+Na$)⁺. **2c:** Yield: 79 %; elemental analyses (C, H and N, wt %) Anal. Calc. for $C_{35}H_{18}N_5O_6BrZn$: C, 56.06; H, 2.42; N, 9.34; found: C, 55.91; H, 2.27; N, 9.54; IR (KBr, cm^{-1}): 2202, $\nu(C\equiv C)$; 1614, $\nu(HC=N)$; 1312, $\nu(C-O)$; 1H NMR (d_6 -DMSO, 300 MHz): δ 9.39 (s, 1H, HC=N), δ 9.14 (s, 1H, HC=N), δ 6.75-8.69 (m, 16H, Ar-H); MS (ESI): m/z 773(M^+). **2d:** Yield: 77%; elemental analyses(C, H and N, wt %) Anal. calc. for $C_{37}H_{24}N_3O_4BrZn$: C, 61.73; H, 3.36; N, 5.84; found: C, 61.56; H, 3.28; N, 5.89; IR (KBr, cm^{-1}): 2199, $\nu(C\equiv C)$; 1615, $\nu(HC=N)$; 1286, $\nu(C-O)$; 1H NMR (d_6 -DMSO, 300 MHz): δ 9.37 (s, 1H, HC=N), δ 9.12 (s, 1H, HC=N), δ 6.71-8.60 (m, 16H, Ar-H), δ 3.74 (s, 6H, OCH_3); MS (ESI): m/z 743 (M^+).

2.4. Kurtz powder SHG measurements

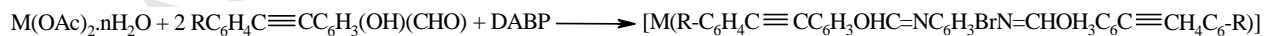
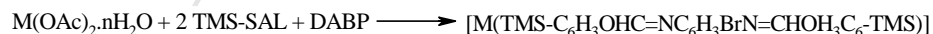
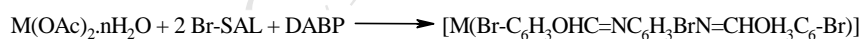
The SHG efficiency of all the complexes was measured with respect to urea by powder technique developed by Kurtz and Perry using Q switched Nd-YAG laser (Lab-170 spectra physics) 10 ns laser with first harmonic output of 1064 nm at the pulse repetition rate 10 Hz. The homogeneous powder was mounted in the path of laser beam of pulse energy 2.2 mJ obtained by split beam technique.

3. Results and discussion

3.1. Synthesis and spectroscopic characterization

The synthetic route to the Ni(II) and Zn(II)-salophen complexes is shown in scheme 1. Initially, 5-(trimethylsilylethylene)salicylaldehyde was prepared by Sonogashira Pd(II)/Cu(I) catalyzed

coupling reaction of 5-bromosalicylaldehyde with trimethylsilylacetylene by following the procedure reported in literature [22]. Removal of trimethylsilyl group in 5-(trimethylsilyl ethylene)salicylaldehyde was achieved by treatment of KOH in methanol to afford 5-ethynyl salicylaldehyde in excellent yield. The compound 5-(4-nitrophenyl)ethynylsalicylaldehyde and 5-(4-methoxyphenyl)ethynylsalicylaldehyde were synthesized by further coupling reactions of 5-ethynylsalicylaldehyde with 1-iodo-4-nitrobenzene and 1-iodo-4-methoxybenzene in THF at 80°C. To explore the influence of π -conjugation and substituent's on phenyl ring of salophen ligand, the complexes **1a**, **2a**, **1b** and **2b** were prepared by following the procedure reported earlier [23] for ease of handling and purification with little modification for which, nickel acetate or zinc acetate was first treated with 5-bromosalicylaldehyde and 5-(trimethylsilylethynyl) salicylaldehyde in THF for 30 min. at room temperature. To the resulting solution was added 2,3-diamino-5-bromopyridine afforded monomeric complexes **1a**, **1b**, **2a** and **2b**, respectively. The complexes **1c**, **1d**, **2c** and **2d** with extended π -conjugation and donor/acceptor substituent's were prepared by treating nickel acetate or zinc acetate with 5-(4-nitrophenyl)ethynyl salicylaldehyde or 5-(4-methoxyphenyl)ethynyl salicylaldehyde then subsequently treated with 2,3-diamino-5-bromopyridine by similar method described above. Complexes **1c** and **2c** with an additional electron-withdrawing NO₂ group whereas, complexes **1d** and **2d** with an electron-donating OCH₃ group on phenylene ring were obtained. The generalized equation for the reaction leading to the formation of the complexes is shown as follows



(where : M=Ni, Zn ; n= 4 (Ni), 2 (Zn) ; Br-SAL= 5-Bromosalicylaldehyde ; TMS-SAL= 5-Trimethylsilylethynylsalicylaldehyde ; R= NO₂, OCH₃ ; DABP= 2,3-diamino-5-bromopyridine)

All complexes were air stable, moisture insensitive and insoluble in common organic solvents except DMF and DMSO. The results of elemental analyses (C, H and N) which are given in section 2 confirm the assigned composition of the complexes.

The IR spectra of **1a-d** and **2a-d** exhibit a medium intensity band due to internal triple bond ($C\equiv C$) observed at $\sim 2145\text{ cm}^{-1}$ [24]. The band observed at $\sim 1610\text{ cm}^{-1}$ in the spectra of **1a-d** and **2a-d** indicate involvement of imine ($HC=N$) nitrogen in coordination with metal ion [25]. This view was further supported by the appearance of a band corresponding to the metal-nitrogen stretching vibration at *ca* $501\text{-}519\text{ cm}^{-1}$ in **1a-d** and *ca* $504\text{-}515\text{ cm}^{-1}$ in **2a-d**. Similarly, another medium intensity band observed at *ca* $1282\text{-}1334\text{ cm}^{-1}$ in **1a-d** and *ca* $1278\text{-}1312\text{ cm}^{-1}$ in **2a-d** is due to $\nu(C-O)$ stretching vibration indicating coordination of the oxygen atom of the phenol group [26]. Further proof for complexation of oxygen is obtained from the appearance of (M-O) band at *ca* $537\text{-}569\text{ cm}^{-1}$ **1a-d** and $543\text{-}564\text{ cm}^{-1}$ **2a-d**. The spectra of **1b** and **2b** exhibit vibrations of Me_3Si at around 1248 and 840 cm^{-1} [27]. Compound **1c** and **2c** exhibit two bands at $\sim 1560\text{ cm}^{-1}$ and $\sim 1400\text{ cm}^{-1}$ which can be attributed to ν_{asym} and ν_{sym} (NO_2) modes, respectively [28]. The strong band at 1244 and 830 cm^{-1} in **1b** and **2b** ascribed to Me_3Si vibration [29]. However, a band at 1167 cm^{-1} in **1d** and 1169 cm^{-1} in **2d** is due to OCH_3 group in the complexes [30].

The 1H NMR spectra of **1a-d** and **2a-d** displayed two resonances for two non-equivalent imine ($HC=N$) protons and appeared at approximately 9.37 and 9.10 ppm confirm the imine nitrogen coordination [31]. The resonance of all aromatic as well as heteroaromatic protons are well resolved and observed at $8.59\text{-}6.65$ ppm in **1a-d** and $8.48\text{-}6.69$ ppm in **2a-d**. In addition to these the resonance at 0.27 ppm in **1b** and **2b** is due to two terminal $Me_3SiC\equiv C$ protons. However, the complexes **1d** and **2d** exhibit resonance at 3.74 ppm for OCH_3 group in the complexes [32].

3.2. Thermo gravimetric analysis

To investigate the thermal stability of Ni(II) (**1a-d**) and Zn(II) (**2a-d**) complexes thermo gravimetric analysis (TGA) were performed up to $800^\circ C$ under nitrogen atmosphere at a heating rate of $10^\circ C\text{ min}^{-1}$. TGA plots suggest that the complexes **1a** and **2a** underwent a weight loss due to the expulsion of water molecules (obsd. 6.11 (**1a**), 6.13 (**2a**)%; cald. 5.93 (**1a**), 5.83 (**2a**)%) in the temperature range between $30\text{-}175^\circ C$ and 32 to $184^\circ C$, respectively. Both the complexes

collapse due to second decomposition stage of coordinated salophen ligand per formula unit which occurs in between 175-749°C and 184-744°C with a significant weight loss of 88.69 (**1a**) and 87.10 (**2a**), respectively (calcd. 88.35 (**1a**) 86.81 (**2a**) %). The decomposition sequence of **1b** and **2b** is similar to that of **1a** and **2a**, once again the loss of water molecule is observed and indicate the decomposition follows the same stages. The first weight loss observed in between 31-183°C and 32-182°C which is presumably due to loss of water molecule (obsd. 5.83 (**1b**), 5.81 (**2b**) %; calcd. 5.58 (**1b**), 5.52 (**2b**)%). The second stage of decomposition with weight loss from 183-753°C (**1b**) and 182-750°C (**2b**) is attributed to the loss of coordinated ligand (obsd. 88.73 (**1b**), 87.80 (**2b**) %; calcd. 88.42 (**1b**), 87.51 (**2b**)%) to give final residue of metal oxide. The TGA curve of **1c**, **2c** and **1d**, **2d** shows similar behavior. In the temperature range 33-176°C and 36-179°C these complexes underwent weight loss corresponds to water molecule (obsd. 5.09 (**1c**), 5.06 (**2c**), 5.32 (**1d**), 5.28 (**2d**); calcd. 4.84 (**1c**), 4.80 (**2c**), 5.05 (**1d**), 5.01 (**2d**)%). All the complexes exhibit weight loss which is assigned to the decomposition of coordinated salophen ligand observed in between 176-764°C (**1c**, **2c**) and 179-766°C (**1d**, **2d**) with an observed weight loss of 90.22 (**1c**), 89.44 (**2c**), 89.84 (**1d**) and 88.96 (**2d**), respectively (calcd. 89.94 (**1c**), 89.14 (**2c**), 89.53 (**1d**), 88,69 (**2d**)%).

3.3. X-ray powder diffraction and SEM studies

Single crystal X-ray diffraction investigation is the most precise source of information regarding the structure of the complexes. However, the difficulties in obtaining crystalline complexes in proper symmetric form has rendered us to perform the powder X-ray diffraction method for such study. The XRPD pattern obtained for the metal complexes **1c** and **2b** revealed well defined crystalline peaks indicating that the complexes **1c** and **2b** is crystalline in phase due to inherent crystalline nature (Fig. 1). The diffractogram of **1c** records thirteen reflections between 5-80° (2 θ) with maximum at 2 θ =18.644° corresponding to value of d=4.755Å (Table 1). The diffractogram of **2b** consists of nine reflections with maxima at 2 θ =18.16° corresponding to value of d=4.879Å (Table 2). The main peaks of **1c** and **2b** have been indexed by using computer

software by trial and error method [33, 34], keeping in mind characteristics of various symmetry systems till good fit could be obtain between observed and calculated 2θ and $\sin^2\theta$ values. The method also yielded hkl values. The relative intensities corresponding to the prominent peaks have been indexed. It was observed that the indexing of the diffractogram of **1c** and **2b** are identical. Based on this it can be proposed that these compounds belong to same structural class. A comparison of values of 2θ and $\sin^2\theta$ for **1c** and **2b** reveals that, there is a good agreement between the calculated and observed values of 2θ and $\sin^2\theta$ on the basis of assumption of monoclinic structure [35]. The structure of **1c** yields values for lattice constant $a=11.1427\text{\AA}$, $b=8.0223\text{\AA}$, and $c=8.9645\text{\AA}$; $\alpha=\gamma=90^\circ$ and $\beta=122.7^\circ$, unit cell volume $V=674.30\text{\AA}^3$. However, the structure of **2b** yields values for lattice constant $a=13.8704\text{\AA}$, $b=9.7067\text{\AA}$ and $c=7.9356\text{\AA}$; $\alpha=\gamma=90^\circ$ and $\beta=99.192^\circ$, unit cell volume $V=1056.69\text{\AA}^3$. In conjunction with these cell parameters the conditions such as $a \neq b \neq c$ and $\alpha=\gamma \neq \beta$ required for the samples to be monoclinic were tested and found to be satisfactory. These results are in good agreement with those are reported in the literature [36, 37]. To explore the morphology and particle size of the prepared complexes the scanning electron micrography (SEM) studies of **1b** and **2d** have been studied and are presented in Fig. 2. The SEM of **1b** seemed of rock like crystals with average size of $\sim 26\text{ }\mu\text{m}$ whereas; the SEM of **2d** shows crystals like nanorods with average size of $\sim 0.9\text{ }\mu\text{m}$.

3.4. Cyclic Voltammetry

The redox properties of Ni(II) complexes were investigated cyclic voltammetrically in DMF solution containing 0.05 M $n\text{-Bu}_4\text{NClO}_4$ as a supporting electrolyte. All measurements were carried out in 10^{-4} M solution at room temperature in the potential range $+1.5$ to -1.5 with scan rate 100 mVs^{-1} . The electrochemical data of the complexes **1a-d** is summarized in Table 3 and representative cyclic voltammogram of **1b** and **1d** are displayed in Fig. 3 and Fig. 4, respectively.

The Ni(II) complexes exhibit a one electron quasireversible oxidation and reduction process. The cyclic voltammetry studies on Ni(II) complexes reveals that all complexes undergoes anodic

processes which is attributed to quasireversible one electron oxidation of Ni(II) to Ni(III) process in the range of 0.890 -0.980 V while cathodic process is attributed to quasireversible one electron reduction Ni(II) to Ni(I) process in the range of -1.227 to -1.369 V, similar to that of observed in other Ni(II)-salopen complexes reported in the literature [38]. The electrochemical data of all the Ni(II) complexes also reveals that the redox responses of Ni(II) complexes shifted to more negative potential in order to increase π -conjugation in the complexes.

3.5. Absorption and emission properties

The UV-Vis absorption spectra of all Nickel(II) (**1a-d**) and Zn(II) (**2a-d**) complexes were measured in DMF solution (10^{-4} M) at room temperature and data are summarized in Table 4. In DMF, the absorption spectra exhibit intense bands at *ca* 235, 285 nm for **1a** and *ca* 245, 275 nm for **2a** which can be assigned to $\pi \rightarrow \pi^*$ and $n \rightarrow \pi^*$ intra-ligand transitions, respectively (Fig. 5). However, a band at 390 nm in **1a** and 440 nm in **2a** assigned to metal to ligand charge transfer (MLCT) transition. Complexes **1b** and **2b** exhibit bands at 236, 290 nm and 240, 295 nm are likely assigned to $\pi \rightarrow \pi^*$ and $n \rightarrow \pi^*$ transition, respectively. Another band at 395 nm in **1b** and 445 nm in **2b** assigned to MLCT transition. In addition to these, a weak absorption at 490 and 505 nm in **1a** and **1b** is due to spin allowed ($^1A_{1g} \rightarrow ^1A_{2g}$) d-d transition having square planar geometry around Ni(II). The observed bathochromic shift in **1b** and **2b** relative to **1a** and **2a** is associated with use of addition of electron donating $C \equiv CSi(CH_3)_3$ moiety in salicylidene ligand resulted in a destabilization of π^* HOMO orbital and a stabilization of LUMO π^* orbital which lead to a smaller HOMO-LUMO energy gap in **1b** and **2b** [39]. The analogous bands are also observed in **1c**, **1d**, **2c** and **2d** with further bathochromic shift. Complexes **1c**, **1d**, **2c** and **2d** exhibit a high intensity band at 235, 245, 236 and 240 which can be assigned to $\pi \rightarrow \pi^*$ transition. Another band at 285 in **1c**, 295 in **1d**, 290 in **2c** and 295 nm in **2d** attributed to $n \rightarrow \pi^*$ transition. However, a band at 415 in **1c**, 440 in **1d**, 441 in **2c** and 447 in **2d** is due to MLCT transition. The spin allowed transition

($^1A_{1g} \rightarrow ^1A_{2g}$) at 525 nm in **1c** and 530 nm in **1d** indicate four coordinate square planer geometry around Ni(II). The observed bathochromic shift in these complexes is associated with increase in π -conjugation and addition of donor-acceptor substituent's in respective complexes

As shown in Fig. 6, the emission observed in **1a-d** and **2a-d** appears to follow the same trend as absorption energy. The complexes **1a** and **2a** exhibit emission at 526 and 531 nm upon excitation at 336 and 328 nm with life time of 1.65 and 1.91 ns, respectively (Table 5). When bromine is replaced by electron donating $C \equiv CSi(CH_3)_3$ forming **1b** and **2b** complexes, the emission are found to be red shifted in comparison to those of **1a** and **2a** and observed at 532 and 538 nm with life time of 1.67 and 1.94 ns, respectively. The complexes **1c** and **2c** shows green emission with maxima at 548 and 564 nm upon excitation at 338 and 341 nm accompanied by life time of 1.69 and 1.96 ns, respectively. However, **1d** and **2d** exhibit emission maxima at 535 and 549 nm excited upon 348 and 358 nm with life time of 1.99 and 1.98 ns, respectively. The emission observed in these complexes confirm that emission origin predominantly not only due to $\pi \rightarrow \pi^*$ intra-ligand transition but also due to some metal to ligand charge transfer (MLCT) character [40]. Compared to **1a**, **1b**, **2a** and **2b** the emission maxima in **1c**, **1d**, **2c** and **2d** are red shifted with increase in life time and such red shift can be related to increase in π -conjugation and donor-acceptor properties of substituted group on coordinated Schiff base ligand. These results might be due to decrease in HOMO-LUMO energy gap and extension of delocalization of the π -electron system along the conjugated backbone in the complexes. With electron withdrawing nitro group on complexes **1c** and **2c** offers an extra conjugated backbone resulting in bathochromic shift (14 nm) in emission spectra relative to **1d** and **2d**. Further, fluorescent intensity is significantly quenched in **1c** and **2c** due to presence of electron withdrawing nitro group in the complexes. These results are in good agreement with those are reported in the literature [41]. The emission quantum yield (ϕ) of all the complexes was determined with reference to quinine sulphate ($\phi = 0.52$) and appeared at 0.194-0.495 for **1a-d** and 0.506-0.537 for **2a-d**. The luminescence decay curve of representative complexes

1a and **2d** are depicted in Fig. 7. The observed decay of the complexes fit well with single exponential decay. Compare to **1a**, **1b**, **2a** and **2b** the average lifetime of **1c**, **1d**, **2c** and **2d** is longer than those observed in **1a**, **1b**, **2a** and **2b** (Table 2). These results could be attributed due to red shifted emission and decreased emission intensity observed in **1c**, **1d**, **2c** and **2d** as compare to **1a**, **1b**, **2a** and **2b**.

The K_r values of **1a-d** and **2a-d** shows marked effect with increase in π -conjugation in the complexes. Further, the highest value of K_r of **1c** and **2c** are results from the cooperative effect of increase in π -conjugation and electron withdrawing NO_2 group on coordinated alkynyl Schiff base ligand.

3.5. SHG activity of the complexes

Nonlinear optical material exhibiting efficient second harmonic generation (SHG) at short wavelengths are important in the field of high density optical recording, laser printing, optical measurement system and for other applications [42, 43]. Among them, new NLO materials made from metal-organic and coordination network have been a major point of focus in recent years to evaluate its potential application as a second-order NLO material [44]. The SHG efficiency of **1a-d** and **2a-d** were screened by the quasi-Kurtz powder technique and the SHG efficiencies relative to the reference (urea) are displayed in Table 6. The comparison of the area of the SHG signal emitted by the sample with the standard urea in the same experimental condition showed that the complexes **1a** and **2a** are 0.19 and 0.21 times that for urea. The complexes **1b** and **2b** are 0.24 and 0.27 times than that of urea. However, **1c**, **1d**, **2c** and **2d** are 0.36, 0.31, 0.34 and 0.28 times that that of urea, respectively. The best values of SHG are found for compound possessing $\text{R}=\text{NO}_2$ group with increased π -conjugation in the coordinated Schiff base ligand that expected on the basis of the electronic asymmetry arguments.

4. Conclusions

This study demonstrates that all the complexes exhibit a distinct MLCT (metal to ligand charge transfer) absorption band and shifted to longer wavelength by increasing π -conjugation in the complexes. Room temperature luminescence is observed for all complexes corresponding to

$\pi \rightarrow \pi^*$ intra-ligand transition with some metal-ligand charge transfer (MLCT) character in DMF and are finely tuned by the degree of extended π -conjugation and variation of the substituent group with different electronic effects in the complexes. The electrochemical behavior of the Ni(II) complexes reveals that the redox responses of all Ni(II) complexes shifted to more negative potential in order to increase π -conjugation in the complexes. The second harmonic generation (SHG) efficiency of the complexes was measured by Kurtz-powder technique indicating that all complexes possess promising potential for the application as a useful nonlinear optical material. Moreover, significant increase in π -conjugation increases SHG efficiency of these complexes.

References:

1. Z.-L. You, H.-L. Zhu, W.-S.Z. Liu, Solvothermal Syntheses and Crystal Structures of Three Linear Trinuclear Schiff Base Complexes of Zinc(II) and Cadmium(II), *Anorg. Allg. Chem.* 630 (2004) 1617.
2. Z.-L. You, H.-L. Zhu, W.-S.Z. Liu, Syntheses, Crystal Structures, and Antibacterial Activities of Four Schiff Base Complexes of Copper and Zinc, *Anorg. Allg. Chem.* 630 (2004) 2754.
3. A. Golcu, M. Tumer, H. Demirelli, R.A. Wheatley, Cd(II) and Cu(II) complexes of polydentate Schiff base ligands: synthesis, characterization, properties and biological activity, *Inorg. Chim. Acta.* 358 (2005)1785.
4. K. E. Splan, A. M. Massari, G. A. Morris, S.-S. Sun, E. Reina, S. T. Nguyen, J. T. Hupp, Photophysical and Energy-Transfer Properties of (Salen)zinc Complexes and Supramolecular Assemblies, *Eur. J. Inorg. Chem.* (2003) 2348.
5. G. A. Morris, H. Zhou, C. L. Stern, S. T. Nguyen, A General High-Yield Route to Bis(salicylaldimine) Zinc(II) Complexes: Application to the Synthesis of Pyridine-Modified Salen-Type Zinc(II) Complexes, *Inorg. Chem.* 40(2001)3222.
6. W.-K. Dong, Y.-X. Sun, Y.-P. Zhang, Li Li, Xue-Ni He, X.-L. Tong., Synthesis, crystal structure, and properties of supramolecular Cu^{II}, Zn^{II}, and Cd^{II} complexes with Salen-type bisoxime ligands, *Inorg. Chim. Acta.* 362 (2009)117.
7. M. Nielsen, N. B. Larsen, K. V. Gothelf, Electron Transfer Reactions of Self-Assembled Monolayers of Thio(Phenylacetylene)_n-Substituted Chiral Metal-Salen Complexes, *Langmuir.* 18 (2002) 27959.
8. S. Chakraborty, C. R. Bhattacharjee, P. Mondal, S. Krishna Prasad, D. S. Shankar Rao, Synthesis and aggregation behaviour of luminescent mesomorphic zinc(II) complexes with 'salen' type asymmetric Schiff base ligands, *Dalton Trans.* 44 (2015)7477.
9. N. Novoa, T. Roisnel, P. Hamon, S. Kahlal, C. Manzur, H. M. Ngo, I. Ledoux-Rak, J.-Y. Saillard, D. Carrillo, J.-R. Hamon, Four-coordinate nickel(II) and copper(II) complex based ONO tridentate Schiff base ligands: synthesis, molecular structure, electrochemical, linear and nonlinear properties, and computational study, *Dalton Trans.* 44(2015)18019.
10. P. G. Lacroix, Second-Order Optical Nonlinearities in Coordination Chemistry: The Case of Bis(salicylaldiminato)metal Schiff Base Complexes, *Eur. J. Inorg. Chem.* (2001) 339.

11. F. Averseng, P. G. Lacroix, I. Malfant, F. Dahan and K. Nakatani, Synthesis, crystal structure and solid state NLO properties of a new chiral bis(salicylaldiminato)nickel(II) Schiff-base complex in a nearly optimized solid state environment, *J. Mater. Chem.* 10 (2000) 1013.
12. I. H. A. Badr, M. E. Meyerhoff, Highly Selective Optical Fluoride Ion Sensor with Submicromolar Detection Limit Based on Aluminum(III) Octaethylporphyrin in Thin Polymeric Film, *J. Am. Chem. Soc.* 127 (2005) 5318.
13. V. Liuzzo, W. Oberhauser, A. Pucci, Synthesis of new red photoluminescent Zn(II)-salicylaldiminato complex, *Inorg. Chem Commun.* 13(2010) 686.
14. T. Feng, H.M. Peng, Y.M. Yao, Y. Zhang, Q. Shen, Y.X. Cheng, Synthesis, characterization and photoluminescence of aluminum *N*-aryloxo functionalized β -ketoiminate complexes, *Chin. Sci. Bull.* 56 (2011)1471.
15. R. Brissos, D. Ramos, J. C. Lima, F. Y. Mihan, M. Borra's, J. de Lapuente, A. Dalla Cort, L. Rodriguez, Luminescent zinc salophen derivatives: cytotoxicity assessment and action mechanism studies, *New J. Chem.* 37(2013)1046.
16. S. Bhattacharjee, K.-E. Jeong, S.-Y. Jeong, W.-S. Ahn, Synthesis of a sulfonato-salen-nickel(II) complex immobilized in LDH for tetralin oxidation, *New J. Chem.* 34(2010)156.
17. A. Zulauf, X. Hong, Brisset, E. Schulz, M. Mellah, Electropolymerization of chiral chromium–salen complexes: new materials for heterogeneous asymmetric catalysis, *New J. Chem.* 36(2012)1399.
18. C. Schmitz, P. Posch, M. Thelakkat, H.-W. Schmidt, A. Montali, K. Felman, P. Smith, C. Weder, Polymeric Light-Emitting Diodes Based on Poly(*p*-phenylene ethynylene), Poly(triphenyldiamine), and Spiroquinoxaline, *Adv. Funct. Mater.* 11(2001) 41.
19. V. W.-W. Yam, K. K.-W. Lo and K. M.-C. Wong, Luminescent polynuclear metal acetylides, *J. Organomet. Chem.* 578(1999) 3.
20. C. Ma, A. Lo, A. Abdol-Maleki, M. J. MacLachalm, Synthesis and Metalation of Novel Fluorescent Conjugated Macrocycles, *Org. Lett.* 6 (2004), 3841.
21. K.-L. Kuo, C.-C. Huang, Y.-C. Lin, Synthesis and photophysical properties of multinuclear zinc-salophen complexes: enhancement of fluorescence by fluorene termini, *Dalton Trans.* (2008)3889.
22. K.-H. Chang, C.-C. Huang, Y.-H. Liu, Y.-H. Hu, P.-T. Chou, Y.-C. Lin, Synthesis of photoluminescent Zn(II) Schiff base complexes and its derivative containing Pd(II) moiety, *Dalton Trans.* (2004)1731.

23. H.-C. Lin, C.-C. Huang, C.-H. Shi, Y.-H. Liao, C.-C. Chen, Y.-C. Lin Y.-H. Liu, Synthesis of alkynylated photo-luminescent Zn(II) and Mg(II) Schiff base Complexes, Dalton Trans. (2007) 781.
24. A. W. C. Leung, M. J. MacLachlan, Poly(salphenyleneethynylene)s: soluble, conjugated metallopolymers that exhibit unique supramolecular crosslinking behavior, J. Mater. Chem. 17 (2007) 1923.
25. M. Mohammadikish, Green synthesis of nanorod Ni(salen) coordination complexes using a simple hydrothermal method, Cryst. Eng. Comm. 16 (2014) 8020.
26. A. Ourari, Y. Ouennoughi, D. Aggoun, M. S. Mubarak, E. M. Pasciak, D. G. Peters, Synthesis, characterization, and electrochemical study of a new tetradentate nickel(II)-Schiff base complex derived from ethylenediamine and 5-(N-methyl-N-phenylaminomethyl)-2'-hydroxyacetophenone, Polyhedron. 67 (2014) 59.
27. M. Shebl, S.M.E. Khalil, S.A. Ahmed, H.A.A. Medien, Synthesis, spectroscopic characterization and antimicrobial activity of mono-, bi- and tri-nuclear metal complexes of a new Schiff base ligand, J. Mol. Struct. 980 (2010) 39.
28. J. Cisterna, V. Dorcet, C. Manzur, I. L.-Rak, J.-R. Hamon, D. Carrillo, Synthesis, spectral, electrochemical, crystal structures and nonlinear optical properties of unsymmetrical Ni(II) and Cu(II) Schiff base complexes, Inorg. Chim. Acta. 430 (2015) 82.
29. H. Balcar, J. Sedlacek, J. Zednik, V. Blechta, P. Kubat, J. Vohlidal, Polymerization of isomeric N-(4-substituted benzylidene)-4-ethynylanilines and 4-substituted N-(4-ethynylbenzylidene)anilines by transition metal catalysts: preparation and characterization of new substituted polyacetylenes with aromatic Schiff base type Pendant groups, Polymer. 42 (2001) 6709.
30. P. Gili, M.G. Martin Reyes, Martin Zarza, I. L. F. Machado, M.F.C. Guedes da Silva, M. A. N. D. A. Lemos A.J. L. Pombeiro, Synthesis, spectroscopic, magnetic and electrochemical properties of Cu(II) and Fe(III) complexes with the new ligand N,N'- [1,1'-dithiobis(phenyl)] bis(5'-methoxysalicylaldehyde), Inorg. Chim. Acta 244 (1996) 25.
31. A. Ourari, K. Ouari, W. Moumeni, L. S. Gilles, M. Bouet, M. A. Khan, Unsymmetrical tetradentate Schiff base complexes derived from 2,3-diaminophenol and salicylaldehyde or 5-bromosalicylaldehyde, Trans. Met. Chem. 31 (2006) 169.
32. S. D. Bella, I. Fragala, A. Guerri, P. Dapporto, K. Nakatani, Synthesis, crystal structure, and second-order nonlinear optical properties of [N, N'-bis(1H-pyrrol-2-ylmethylene)-1,2-benzenediaminato]nickel(II) Schiff base complexes, Inorg. Chim. Acta 357(2004) 1161.

33. D. Kivelson, R. Neiman, ESR Studies on the Bonding in Copper Complexes, *J. Chem. Phys.* 35(1961) 149.
34. A. Boultif, D. Louer, Powder pattern indexing with the dichotomy method, *J. Appl. Cryst.* 37(2004) 724.
35. C. R. Bhattacharjee, G. Das, P. Mondal, Photoluminescent Hemidisc-Shaped Liquid Crystalline Nickel(II) Schiff-Base Complexes, *Eur. J. Inorg. Chem.* (2011) 5390.
36. C. R. Bhattacharjee, G. Das, P. Mondal, S. K. Prasad, D. S. Shankar Rao, Novel Green Light Emitting Nondiscoid Liquid Crystalline Zinc(II) Schiff Base Complexes, *Eur. J. Inorg. Chem.* (2011) 1418.
37. F. Morale, R. W. Date, D. Guillon, D. W. Bruce, R. L. Finn, C. Wilson, A. J. Blake, M. Schroder, B. Donnio, Columnar Mesomorphism from Hemi-Disklike Metallomesogens Derived from 2,6-Bis[3',4',5'- tri(alkoxy)phenyliminomethyl]pyridines (L): Crystal and Molecular Structures of [M(L)Cl₂](M= Mn, Ni, Zn), *Chem. Eur. J.* 9 (2003) 2484.
38. A. Anthonysamy, S. Balsubramaniam, Synthesis, spectral, thermal and electrochemical studies of nickel (II) complexes with N₂O₂ donor ligands, *Inorg. Chem. Commun.* 8(2005) 908.
39. W. Yang, W. Yang, W. Li, W. Qin, Study on the synthesis, characterization, photophysical performance and oxygen-sensing behavior of a luminescent Cu(I) complex with large conjugation plane, *Spectrochim. Acta. Part A.* 104(2013) 56.
40. N. J. Turro, Energy Transfer Processes, *Pure Appl. Chem.* 49(1977) 405.
41. R. D. Archer, H. Chen, L. C. Thompson, Synthesis, Characterization, and Luminescence of Europium(III) Schiff Base Complexes, *Inorg. Chem.* 37(1998) 2089.
42. J. Zyss, I. Ledoux, Nonlinear Optics in Multipolar Media: Theory and Experiments, *Chem. Rev.* 94(1994) 77.
43. T. Verbiest, S. Houbrechts, M. Kauranen, A. Persoons, Second-order nonlinear optical materials: recent advances in chromophore design, *J. Mater. Chem.* 7(1997) 2175.
44. S. D. Bella, Second-order nonlinear optical properties of transition metal Complexes, *Chem. Soc. Rev.* 30(2001) 355.

Figure captions:

Scheme 1: Synthetic route to the complexes **1a-d** and **2a-d**

Fig. 1: X-ray diffractogram of (A) **1c** and (B) **2b**

Fig. 2: Scanning electron micrographs of (A) **1b** and (B) **2d**

Fig. 3: Cyclic voltammogram of **1b** in DMF (A) reduction potential (B) oxidation potential

Fig. 4: Cyclic voltammogram of **1d** in DMF (A) reduction potential (B) oxidation potential

Fig. 5: Electronic Absorption Spectra of complexes (A) **1a-d** and (B) **2a-d**

Fig. 6: Emission spectra of complexes (A) **1a-d** and (B) **2a-d**

Fig. 7: Luminescence decay of (A) **1c** and (B) **2d**

Table 1: X-ray diffraction data of **1c**

d (Å)	I/I_0	$\sin^2\theta$ Obs.	$\sin^2\theta$ Calc.	hkl	2θ Obs.	2θ Calc.
8.0223	31.38	92.2	92.2	010	11.02	11.02
6.0956	12.33	159.7	159.7	110	14.52	14.52
5.4955	13.18	196.5	196.5	011	16.11	16.11
4.7551	100	262.4	262.4	101	18.64	18.64
4.4066	28.74	305.5	303.3	-102	20.13	20.06
4.0695	14.51	358.3	354.6	111	21.82	21.71
3.8754	17.45	395.0	395.4	-112	22.93	22.94
3.2586	49.11	558.7	561.7	-221	27.35	27.42
3.1359	29.64	603.3	607.4	300	28.44	28.53
2.9217	13.8	695.0	693.2	-222	30.57	30.53
2.7016	14.6	812.9	808.5	-321	33.13	33.04
2.5131	10.36	939.4	938.4	003	35.70	35.68
1.9940	4.98	1492.1	1494.2	-223	45.45	45.48

Table 2: X-ray diffraction data of **2b**

d (Å)	I/I_0	$\sin^2\theta$ Obs.	$\sin^2\theta$ Calc.	hkl	2θ Obs.	2θ Calc.
7.9187	42.64	94.6	94.6	110	11.16	11.16
7.3223	23.05	110.7	110.7	-101	12.08	12.08
6.3747	11.31	146.0	146.0	101	13.88	13.88
5.6189	39.82	187.9	187.9	-201	15.76	15.76
4.8799	88.21	249.1	250.9	-211	18.16	18.23
4.7748	77.47	260.2	258.6	201	18.57	18.51
4.2961	21.58	321.5	321.6	211	20.66	20.66
3.6424	18.29	447.2	446.0	-112	24.42	24.38
3.3327	100	534.2	532.3	-401	26.73	26.68

Table 3: Electrochemical data of Ni(II) complexes (**1a-d**) in DMF

Compound	Oxidation Potentials			Reduction Potentials			
	E_{pa} (V)	E_{pc} (V)	$E_{1/2}$ (V) ΔE_p (mV)	E_{pa} (V)	E_{pc} (V)	$E_{1/2}$ (V) ΔE_p (mV)	
1a	0.890	0.765	0.827(169)	-1.353	-1.227	-1.290(126)	
1b	0.901	0.751	0.826(150)	-1.315	-1.249	-1.282(66)	
1c	0.980	0.721	0.850(269)	-1.277	-1.340	-1.308(63)	
1d	0.942	0.690	0.816(252)	-1.254	-1.369	-1.311(115)	

Table 4: UV-Visible data of **1a-d** and **2a-d** in DMF

Complex	λ_{max} (nm)($\epsilon \times 10^4, M^{-1} cm^{-1}$)
1a	235(28.9), 285(21.1), 390(15.1), 490(9.2)
1b	236(27.5), 290(19.8), 395(11.6), 505(7.5)
1c	235(25.8), 285(18.1), 415 (9.2), 525(4.2)
1d	245(25.2), 295(17.5), 440(8.7), 530(3.6)
2a	245(34.5), 275(16.6), 440(16.7)
2b	240(32.5), 295(23.5), 445(12.5)
2c	236(27.6), 290(20.8), 441(16.1)
2d	240(21.5), 295(18.8), 447(14.9)

Table 5: Photoluminescence data of **1a-d** and **2a-d** in DMF

Complex	λ_{ex} (nm)	λ_{em} (nm)	ϕ	τ (ns)	K_r ($\text{s}^{-1}/10^7$)	K_{nr} ($\text{s}^{-1}/10^7$)
1a	336	526	0.194	1.65	0.117	0.488
1b	340	532	0.298	1.67	0.178	0.420
1c	338	548	0.430	1.69	0.254	0.338
1d	348	535	0.495	1.99	0.248	0.254
2a	328	531	0.506	1.91	0.265	0.258
2b	338	538	0.520	1.94	0.268	0.247
2c	341	564	0.535	1.96	0.272	0.242
2d	358	549	0.537	1.98	0.271	0.234

Table 6: Measured SHG values of **1a-d** and **2a-d**

Complex	Efficiency (relative to urea)
1a	0.19
1b	0.24
1c	0.36
1d	0.31
2a	0.21
2b	0.27
2c	0.34
2d	0.28

Scheme 1

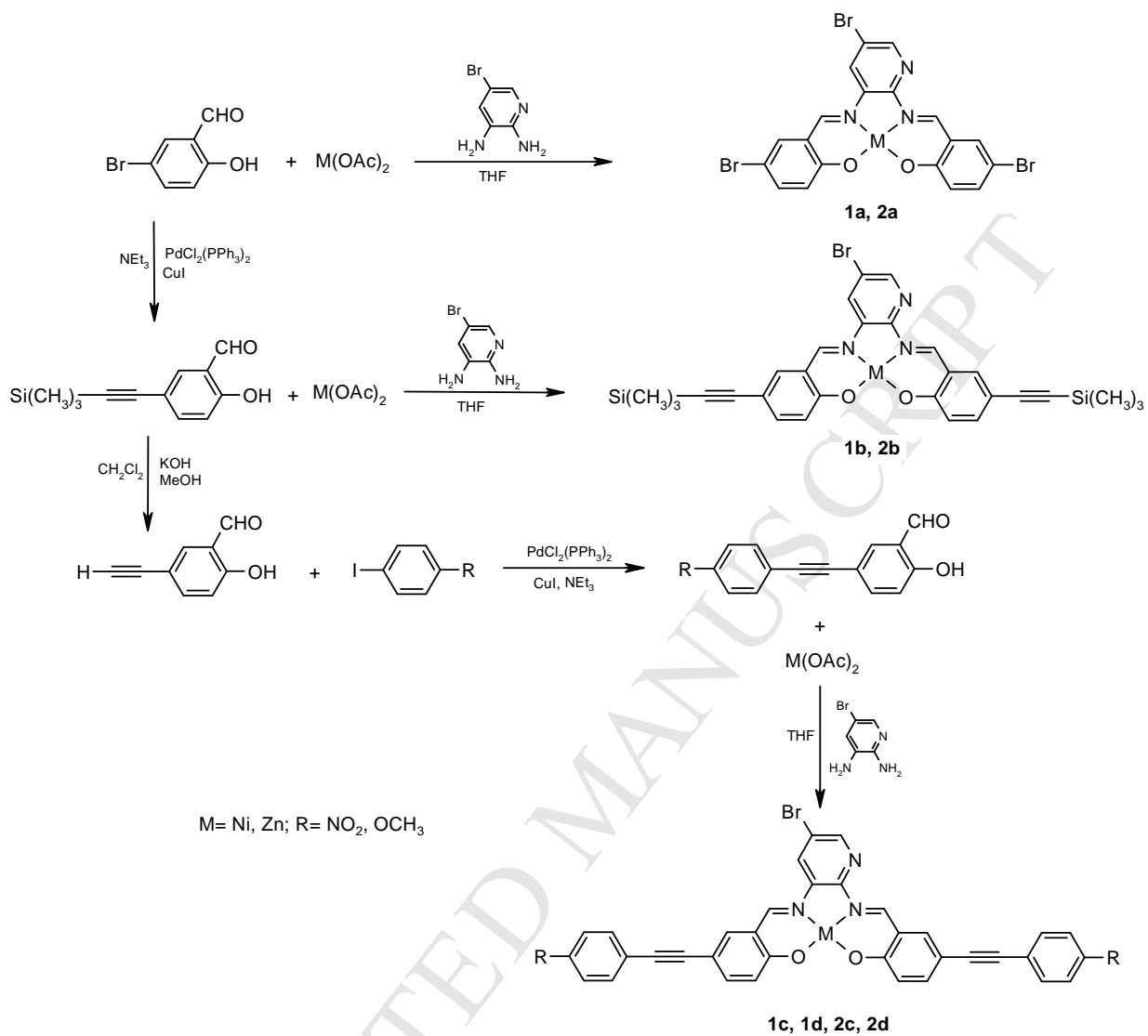


Fig. 1:

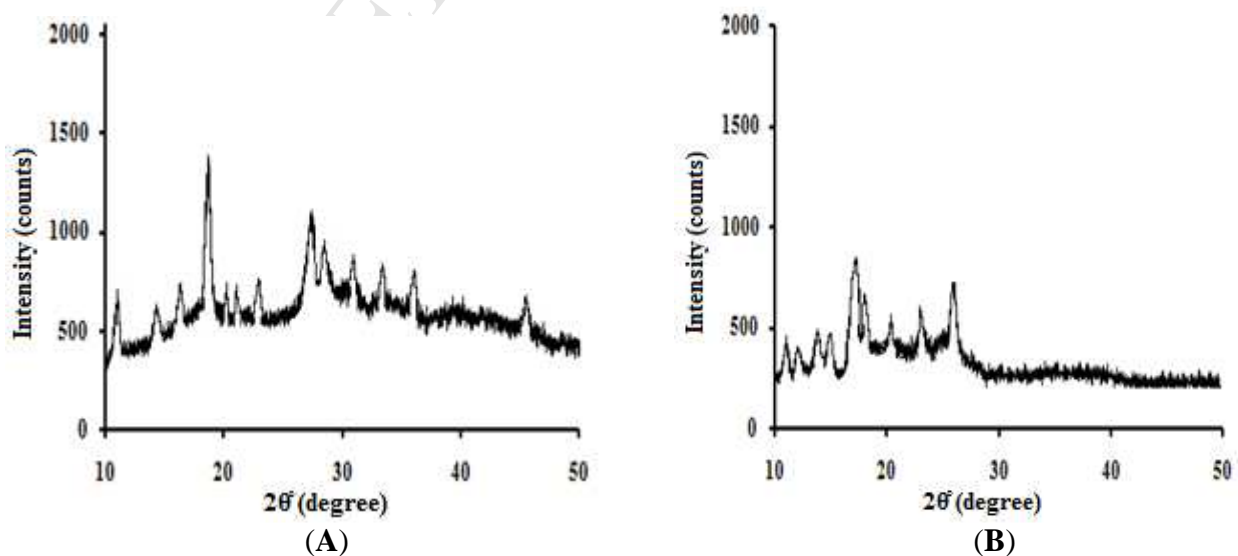


Fig. 2:

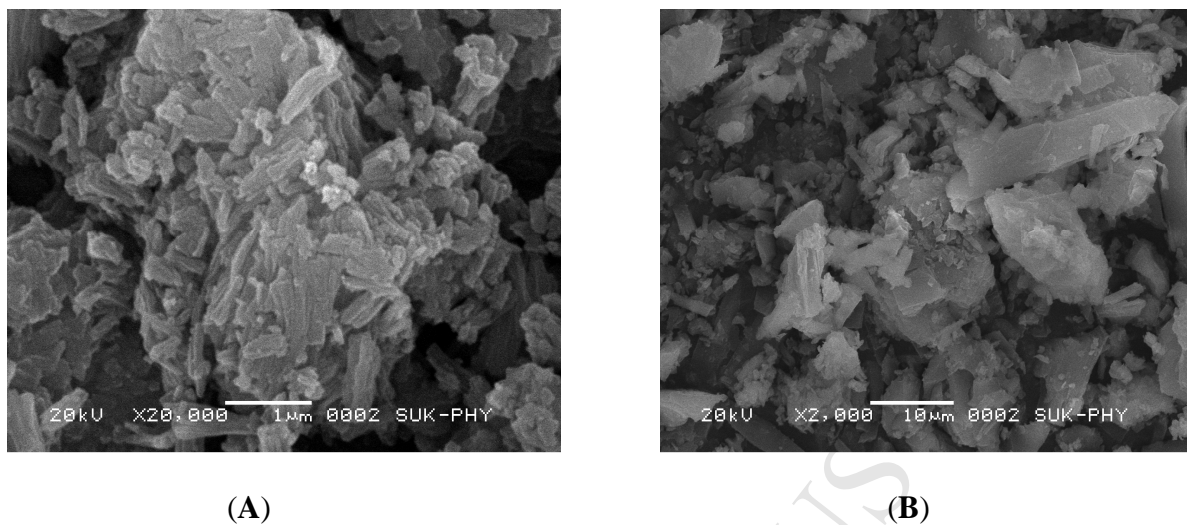


Fig. 3:

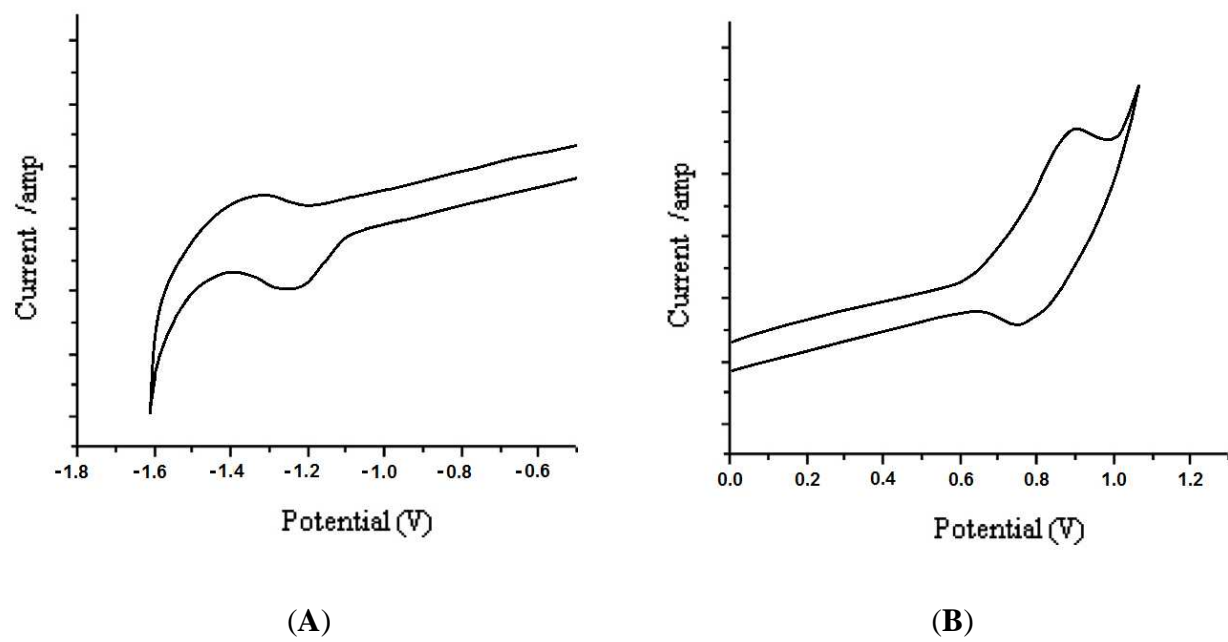


Fig. 4:

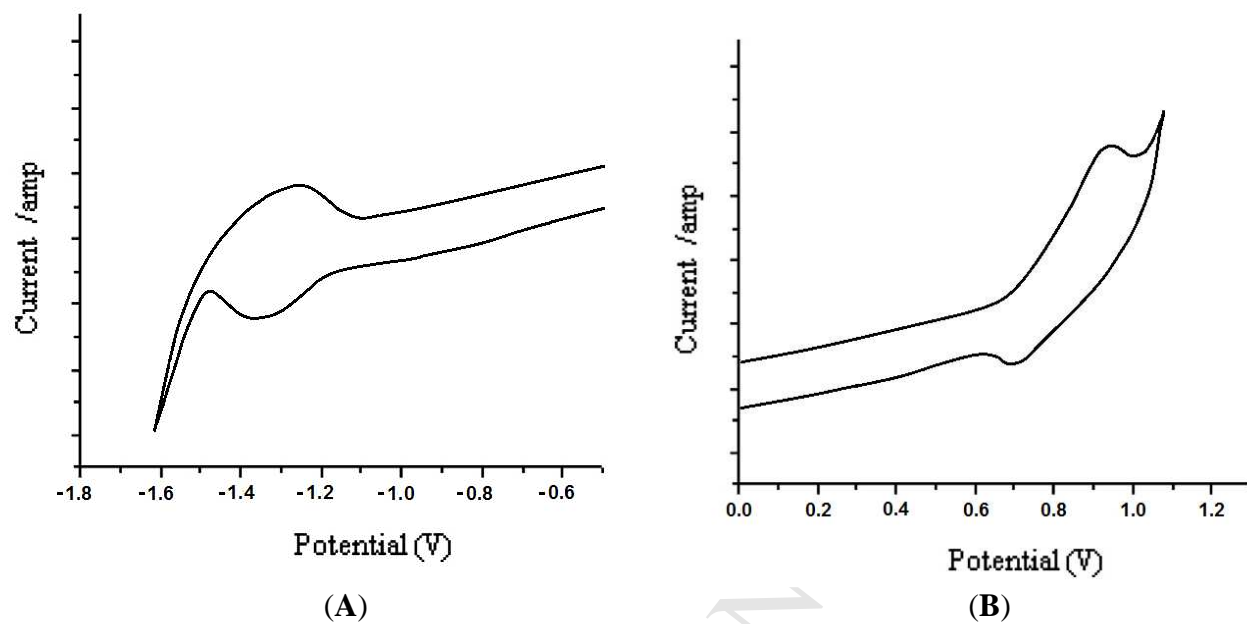


Fig. 5:

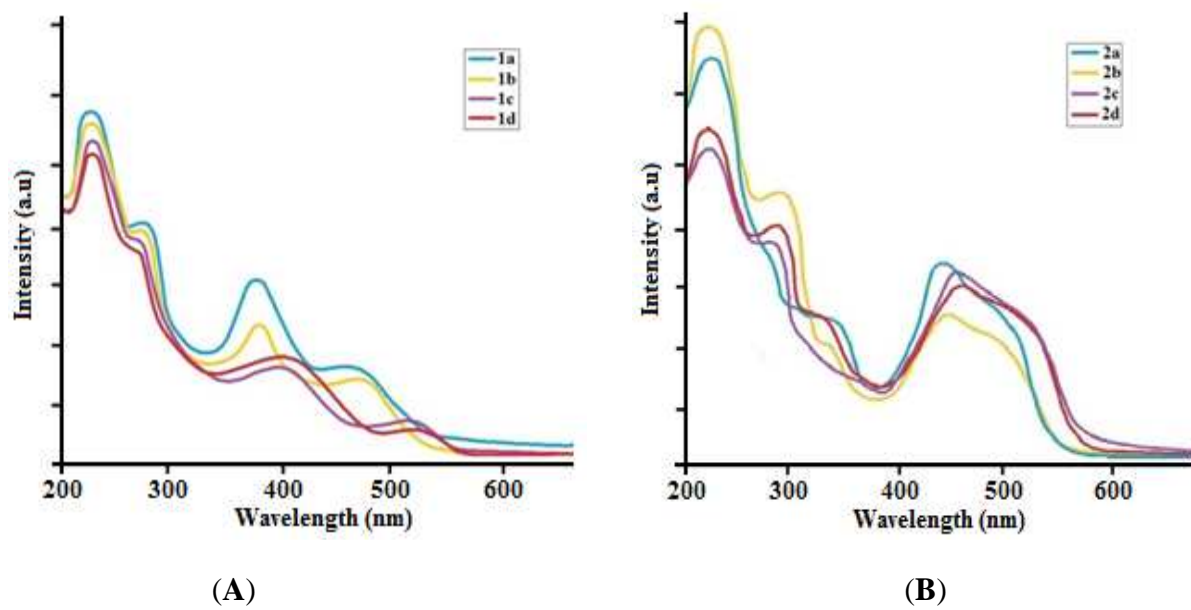


Fig. 6:

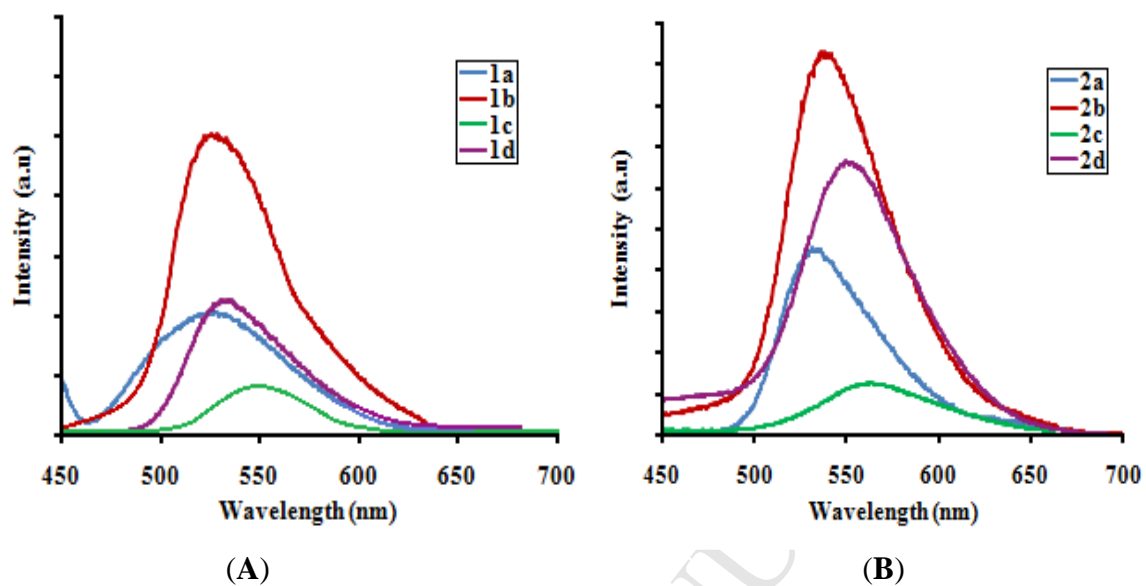
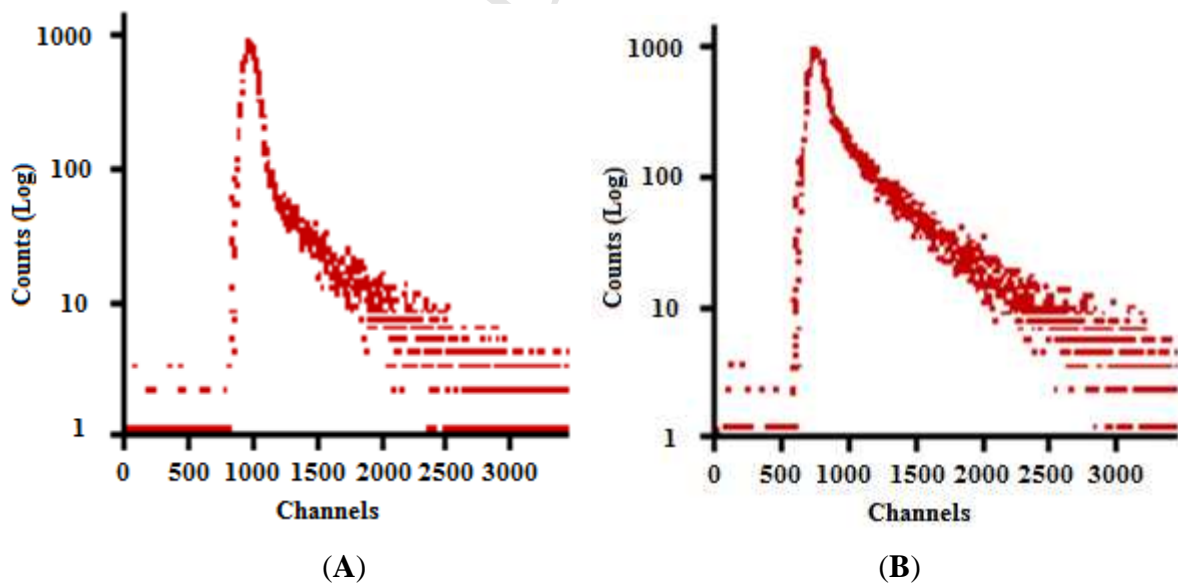


Fig. 7:



Research Highlights:

- Synthesis of Ni(II), Zn(II)-Salophen complexes
- Characterization by elemental analyses, IR, ^1H NMR and mass spectral studies
- Room temperature luminescence is observed for all complexes
- All complexes possess potential application as a useful NLO material.